Single-cell transcriptomic profiling redefines the origin and specification of early adrenogonadal progenitors

Yasmine Neirijnck, Pauline Sararols, Françoise Kühne, Chloé Mayère, Lahiru Chamara Weerasinghe Arachchige, Violaine Regard, Serge Nef, Andreas Schedl

Cell Reports

Resource

Single-cell transcriptomic profiling redefines the origin and specification of early adrenogonadal progenitors

Graphical abstract

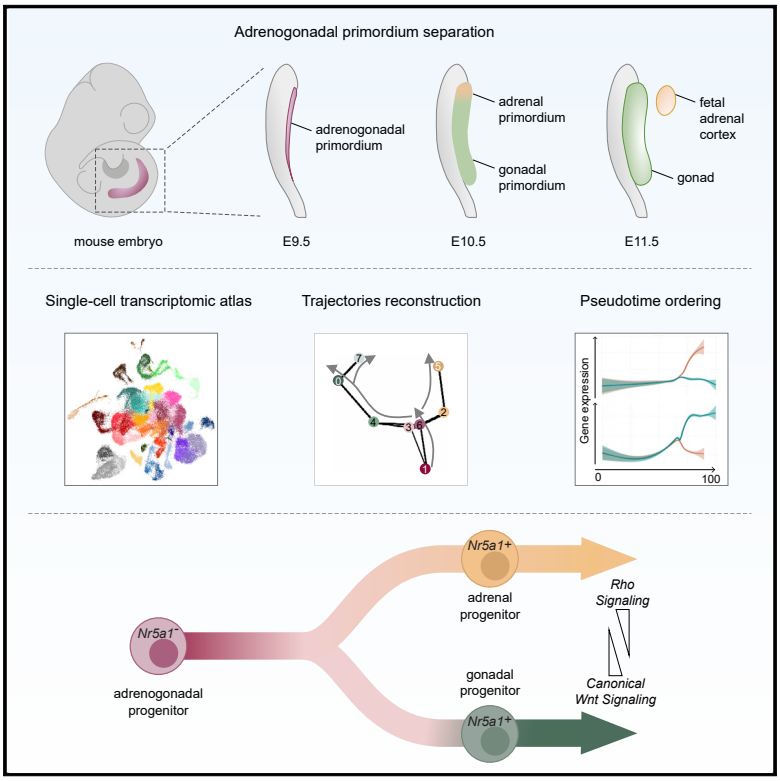

Highlights

- A comprehensive scRNA-seq atlas of early mouse adrenogonadal development
- Mouse adrenogonadal progenitors originate from the lateral plate mesoderm
- Gonadal and adrenal progenitors are specified prior to *Nr5a1* expression
- Gonadal versus adrenal fate involves canonical versus non-canonical Wnt signaling

Authors

Yasmine Neirijnck, Pauline Sararols, Françoise Kühne, ..., Violaine Regard, Serge Nef, Andreas Schedl

Correspondence

yasmine.neirijnck@univ-cotedazur.fr (Y.N.),
serge.nef@unige.ch (S.N.),
andreas.schedl@univ-cotedazur.fr (A.S.)

In brief

Neirijnck et al. report a high-resolution single-cell atlas of early mouse adrenogonadal development. Their analysis demonstrates that gonadal and adrenal progenitors derive from the lateral, rather than the intermediate, mesoderm and are specified before *Nr5a1* expression. While gonadal cells activate the canonical Wnt pathway, adrenal cells show enhanced Rho signaling.

Neirijnck et al., 2023, Cell Reports *42*, 112191
March 28, 2023
https://doi.org/10.1016/j.celrep.2023.112191

CellPress

Cell Reports

CellPress
OPEN ACCESS

Resource

Single-cell transcriptomic profiling redefines the origin and specification of early adrenogonadal progenitors

Yasmine Neirijnck,[1,2,3,*] Pauline Sararols,[1,3] Françoise Kühne,[1] Chloé Mayère,[1] Lahiru Chamara Weerasinghe Arachchige,[2] Violaine Regard,[1] Serge Nef,[1,4,*] and Andreas Schedl[2,*]

[1]Department of Genetic Medicine and Development, University of Geneva, 1211 Geneva, Switzerland
[2]Université Côte d'Azur, CNRS, INSERM, IBV, 06108 Nice, France
[3]These authors contributed equally
[4]Lead contact
*Correspondence: yasmine.neirijnck@univ-cotedazur.fr (Y.N.), serge.nef@unige.ch (S.N.), andreas.schedl@univ-cotedazur.fr (A.S.)
https://doi.org/10.1016/j.celrep.2023.112191

SUMMARY

Adrenal cortex and gonads represent the two major steroidogenic organs in mammals. Both tissues are considered to share a common developmental origin characterized by the expression of *Nr5a1/Sf1*. The precise origin of adrenogonadal progenitors and the processes driving differentiation toward the adrenal or gonadal fate remain, however, elusive. Here, we provide a comprehensive single-cell transcriptomic atlas of early mouse adrenogonadal development including 52 cell types belonging to twelve major cell lineages. Trajectory reconstruction reveals that adrenogonadal cells emerge from the lateral plate rather than the intermediate mesoderm. Surprisingly, we find that gonadal and adrenal fates have already diverged prior to *Nr5a1* expression. Finally, lineage separation into gonadal and adrenal fates involves canonical versus non-canonical Wnt signaling and differential expression of *Hox* patterning genes. Thus, our study provides important insights into the molecular programs of adrenal and gonadal fate choice and will be a valuable resource for further research into adrenogonadal ontogenesis.

INTRODUCTION

Steroids are essential hormones, regulating a wide variety of developmental and physiological processes including reproduction, blood pressure, and the response to stress and infections. The two main steroidogenic organs in mammals, the adrenal cortex and the gonads (testis and ovary), are thought to share a common developmental origin, the adrenogonadal primordium (AGP). In mice, the AGP is specified at around embryonic day 9 (E9)-E10 at the interface of the lateral plate and intermediate mesoderm and is characterized by the expression of the transcription factors *Wt1*, *Gata4*, and *Lhx9* and the nuclear steroidogenic factor 1 (*Sf1*; also named *Nr5a1* or *Ad4BP*).[1–3] The AGP is composed of multipotent cells that, by E10.5, differentiate into the adrenal primordium (AP) and the gonadal primordium (GP).[4] As the AGP grows and expands, NR5A1$^+$ cells delaminate from the coelomic epithelium (CE) and invade the underlying mesenchyme. Ingressing NR5A1$^+$ cells along the rostral-caudal axis contribute to the formation of the GP. Around E11.5, the bipotential GP initiates its differentiation program according to its chromosomal sex toward testicular or ovarian fate. In contrast, the more medial NR5A1$^+$ cells located in the rostral region of the AGP migrate to the cranial end of the mesonephros to form the AP. GP and AP cells can be distinguished transcriptionally based on the expression of *Wt1* and *Gata4* that are downregulated in the AP shortly after separation.[5] By E11.5, the AP differentiates as a steroidogenic fetal zone, and surrounding mesenchymal cells begin to condense around the primordium that, by E12.5–E14.5, will have formed the adrenal capsule.[6]

Despite considerable efforts, the composition and identity of early adrenogonadal progenitors, as well as the transcriptional events that determine their specification and differentiation toward an adrenal or gonadal fate, remain poorly characterized. Furthermore, how the AGP is specified within the mesoderm remains controversial. *Nr5a1* expression analyses and cell lineage-tracing studies in chicken have shown that AGP cells originate from the nephrogenic mesenchyme derived from the intermediate mesoderm (IM),[7,8] a concept recently supported by a single-cell transcriptomic study.[9] In contrast, in mammals, *Nr5a1*$^+$ AGP cells are first observed in the lateral plate mesoderm (LPM)-derived CE,[1,4] a compartment that contributes to somatic cells of the gonad.[10,11] However, a recent single-cell transcriptomic analysis of isolated *Osr1*-GFP$^+$ cells in mice argues for an IM origin of early adrenogonadal progenitors,[12] highlighting that the ontogeny of the mammalian AGP remains unclear. Here, we generated an unbiased and comprehensive single-cell transcriptomic atlas of early mouse adrenogonadal development from E9 to E12.5. This atlas allowed us to characterize the progenitor cells present in the AGP, map their ontogeny, and characterize the lineage specification and differentiation toward adrenal and gonadal primordia.

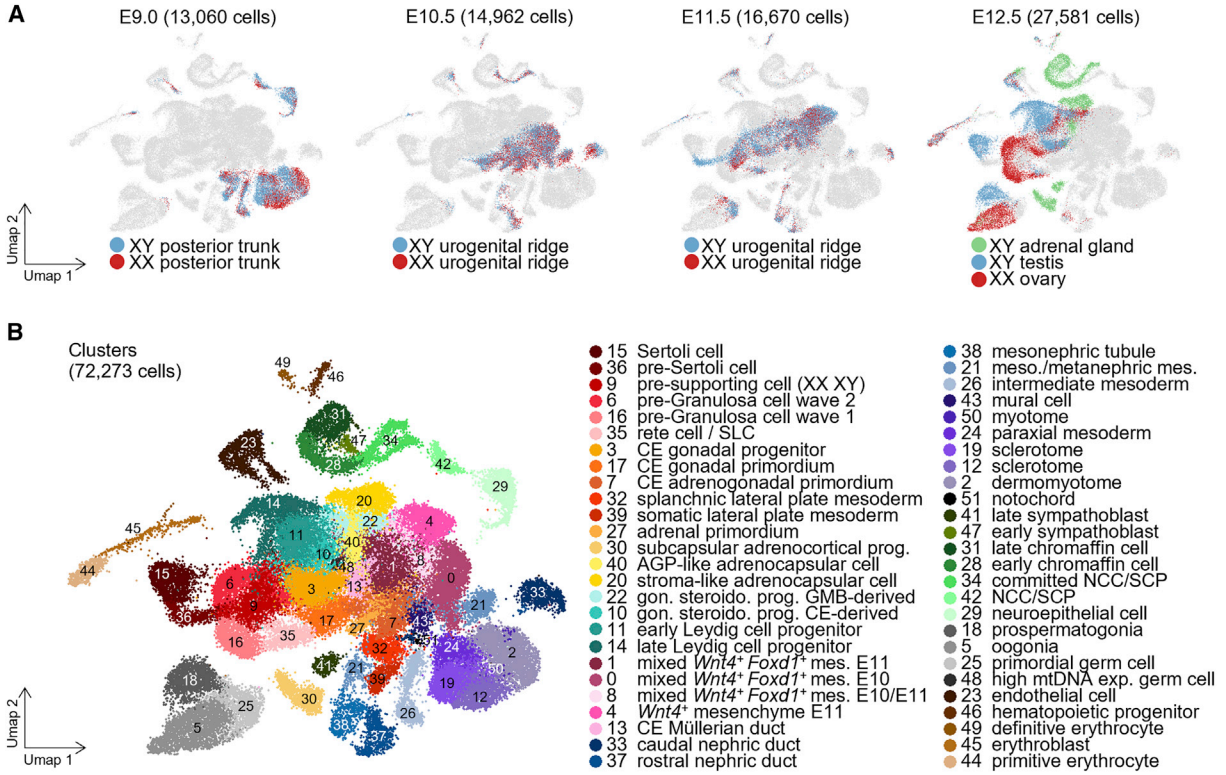

(legend on next page)

RESULTS

A single-cell transcriptomic atlas of early adrenogonadal development

To generate a gene expression atlas of early adrenogonadal development, we performed single-cell transcriptome profiling using a high-throughput droplet-based system (10X Genomics). Single cells were isolated at the time of AGP specification (E9), AGP separation (E10.5), gonadal sex determination (E11.5), and subsequent differentiation (E12.5)[1,13] from *Nr5a1-EGFP*^{Tg} mouse embryos. This transgene expresses *EGFP* under the control of 50 kilobases of the *Nr5a1* promoter,[14] allowing easy visualization during dissections. Of note, EGFP was not used to isolate cells by fluorescence-activated cell sorting (FACS), and entire dissociated organs were processed for single-cell library preparation. Entire posterior trunks (E9), urogenital ridges (E10.5 and E11.5), and gonads (E12.5) were isolated from XY and XX embryos. Adrenals glands (E12.5) were harvested only from XY embryos. Our dataset includes a total of 72,273 cells and 18,913 genes, with a median of 20,260 unique transcripts (UMIs) per cell, 4,558 genes per cell, and 4.5 UMIs/gene per cell (Figures S1A and S1B). Visualization of the single-cell transcriptomes in a uniform manifold approximation and projection (UMAP) space[15] shows that while male and female cells overlap at early stages, a subset of male cells emerges at E11.5, concomitant with gonadal sex determination (Figure 1A).[13] By E12.5, the cells comprising the developing ovaries, testes, and adrenal glands are clearly separated, reflecting diversification of the adrenogonadal cell types (Figure 1A). We applied unsupervised clustering (see STAR Methods) to classify cells based on transcriptomic similarities, resulting in 52 clusters (labelled C0 to C51; Figure 1B). Differential expression analysis identified specific or enriched genes in each cluster that were subsequently cross-referenced with previously established markers (Table S1). Cell types were assigned manually using *a priori* knowledge, combining expression of known specific/enriched marker genes, developmental age, sex, and sample origin of the cells (Figures 1B, 1C, S1C, S1D, and S2; Table S1). We mapped the 52 clusters (hereafter abbreviated as C) into 12 major lineages (Figures 1C and S2): hematopoietic/endothelial, germ cells, neural/sympathoadrenal, notochord, paraxial mesoderm, nephrogenic, mesonephros-associated cell types, gonadal steroidogenic, adrenal steroidogenic, LPM, adrenogonadal progenitors, and supporting cell lineages.

Adrenogonadal progenitors were identified by the expression of early adrenogonadal markers (*Gata4*, *Lhx9*, *Nr5a1*) together with CE markers (*Upk3b*,[16] *Myrf*[17]) (Figures 1C and S2B). This population is composed of cells of both sexes from E10.5 (C17) and from E11.5/E12.5 (C3) (Figures 1A, S1C, and S1D), annotated as "coelomic epithelium gonadal primordium" and "coelomic epithelium gonadal progenitor," respectively. The fate of CE progenitors has been shown to differ before and after E11.2, with early cells preferentially giving rise to supporting cells, whereas later cells fuel the steroidogenic lineage.[10,11] In agreement with this work, early and late CE cells in our dataset were found to be transcriptionally distinct, and CE cells at E11.5/E12.5 cluster close to the steroidogenic lineage. An additional population of *Gata4*$^{+}$/*Lhx9*^{low}/*Upk3b*^{low}/*Myrf*$^{+}$ cells (Figures 1C and S2B) are present at E10.5 (C7) (Figures 1A and S1C). *Nr5a1*, whose expression is known to be downstream of *Gata4* and *Lhx9,* is scarcely detected in this cluster.[2,3,18] C7 thus corresponds to newly specified adrenogonadal cells and is annotated "coelomic epithelium adrenogonadal primordium."

The supporting cell lineage comprises XY *Sox9*$^{+}$/*Ptgds*^{low} pre-Sertoli and *Sox9*$^{+}$/*Ptgds*^{high} Sertoli cells (C36 and C15, respectively), *Gadd45g*$^{+}$ pre-supporting cells originating from both sexes at E11.5 (C9), and two clusters consisting of E12.5 ovary cells expressing the pre-Granulosa cell markers *Irx3* and *Fst* (C6 and C16) (Figures 1A–1C, S1C, S1D, and S2A). While C16 preferentially expresses *Foxl2*/*Hmgcs2*/*Akr1cl*, C6 expresses higher amounts of *Lhx9*/*Gng13* (Figures 1C and S2A and Table S1), which correspond to the first and second wave of pre-Granulosa cells recently described in.[19] C35 contains cells of both sexes at E11.5/E12.5 (Figures 1A, S1C, and S1D), co-expresses *Nr5a1* and *Sox9*, as well as *Pax8* (Figures 1C and S2B), and is therefore referred to as "rete cell/supporting-like cell (SLC)"[20,21] at the origin of the rete testis and rete ovarii.[22]

Progenitors of the gonadal steroidogenic lineage were identified by *Arx* expression[23] (Figure 1C). *Insl3*$^{-}$ C11 and *Insl3*$^{+}$ C14 (Figures 1C and S2E) were exclusively composed of testicular cells at E12.5 (Figures 1A, S1C, and S1D) and were therefore referred to as early and late Leydig cell progenitors, respectively. C10 and C22, on the other hand, were derived from both sexes (Figures 1A and S1D) and express different levels of *Lhx9*, *Mafb*, and *Maf*[11] (Figure 1C). *Lhx9*$^{+}$/*Mafb*^{high}/*Maf*^{low} C10 is therefore annotated as "gonadal steroidogenic progenitor coelomic epithelium-derived," whereas *Lhx9*$^{-}$/*Mafb*^{low}/*Maf*^{high} C22 is referred to as "gonadal steroidogenic progenitor gonad/mesonephros border-derived."

The adrenal steroidogenic lineage contains *Nr5a1*$^{+}$ steroidogenic cells at E12.5 (Figures S2B, 1A, 1C, and S1C) that co-express adrenal-specific genes (*Mc2r*, *Cyp21a1*) (Figure 1C) and adrenal steroidogenic progenitor markers (*Wnt4*, *Shh*^{low}, *Gli1*^{low}) (Figures 1C, S2D, S2F, and S2I); thus, they have been named "subcapsular adrenocortical progenitor" (C30).[24] Adrenal gland samples at E12.5 also contain two *Nr5a1*$^{-}$/*Gli1*$^{+}$/*Ptch1*$^{+}$/*Rspo3*$^{+}$ non-steroidogenic populations (Figures S2B, S2D, and 1C) that could likely represent SHH-responsive capsular steroidogenic progenitors (C20 and C40).[24] While C40 displays an early adrenogonadal transcriptomic signature (*Lhx9*, *Gata4*, *Nr0b1*)

Figure 1. A single-cell transcriptomic atlas of early adrenogonadal development

(A and B) UMAP visualization of the 72,273 transcriptomes colored by age, sex, sample type (A), and by clusters (B). Cell type annotation is shown on the right. AGP, adrenogonadal primordium; CE, coelomic epithelium; GMB, gonad/mesonephros border; gon. steroido. prog., gonadal steroidogenic progenitor; mes., mesenchyme; meson., mesonephric; mtDNA exp., mitochondrial DNA expressing; NCC, neural crest cell; SLC, supporting-like cell; SCP, Schwann cell precursor.

(C) Dot plot showing expression of selected marker gene (x axis) per cluster (y axis). The size of the dot represents the percentage of cells in the cluster expressing the gene, and the color indicates the level of expression (log normalized counts). Major cell lineages are displayed on the left (see also Figures S1 and S2).

(Figures 1C, S2B, and S2D), C20 cells express higher levels of capsular genes *Tcf21* and *Wt1*[5,25] and stromal genes (*Foxd1*, *Dcn*, *Olfml3*) (Figures S2D, S2E, S2F, and 1C; Table S1). C40 and C20 were therefore annotated as "adrenogonadal-like adrenocapsular cells" and "stroma-like adrenocapsular cells," respectively. The fact we could detect two adrenal capsular clusters in our atlas is in line with the known cell type diversification of the capsule. Indeed, lineage-tracing experiments have shown the adrenal capsule to be derived from *Wt1*$^+$ mesenchymal cells,[5] which can be functionally subdivided into *Gli1*$^+$ and *Tcf21*$^+$ progenitors of steroidogenic and stromal lineage, respectively.[24,25] While both cell populations express *Gli1*, C20 expresses higher levels of *Tcf21* and may represent progenitors of non-steroidogenic interstitial lineage. The AP is identified at E10.5 by *Nr5a1*$^+$ cells (Figures 1A, S1C, and S2B) and differs from the GP by its low expression level of *Wt1*/*Gata4*/*Nr0b1* (C27)[5,26] (Figures 1C, S2B, and S2D). This cluster expresses *Mc2r*, *Star*, and *Mgarp* (Figures 1C and S2D), indicating that a steroidogenic transcriptional program is already initiated at this early stage.

The hematopoietic/endothelial lineage contains *Klf1*$^+$ erythroblasts (C45), *Hbb-bh1*$^+$/*Hba-a2*$^+$ primitive and *Hbb-bh1*$^-$/*Hba-a2*$^+$ definitive erythrocytes (C44 and C49, respectively), *Ptprc*$^+$/*Runx1*$^+$ hematopoietic progenitors (C46), and *Cdh5*$^+$ endothelial cells (C23) (Figures 1C and S2L).

Germ cells were identified by *Pou5f1* expression and consisted of several clusters, one of which contained primordial germ cells of both sexes (C25) (Figures 1A–1C and S1D). C18 and C5 contained sex-enriched E12.5 cells, corresponding to *Lefty1*$^+$ prospermatogonia and *Stra8*$^+$ oogonia, respectively (Figures 1A–1C and S1D). Another germ cell population with higher mitochondrial gene expression clustered separately (C48) (Figures 1C and S1B) and could correspond to the nurse/dying cells described in mouse fetal ovaries by Niu and Spradling.[19] Cells of these four clusters are part of the dataset previously analyzed in Mayère et al.[27]

The neural/sympathoadrenal lineage contains E9 *Foxb1*$^+$ neuroepithelial cells (C29), E9 *Plp1*$^+$ neural crest cells (NCCs)/Schwann cell precursors (SCPs) (C42), and *Plp1*$^+$ NCCs/SCPs expressing both a sympathetic progenitor marker (*Ret*) and an SCP-to-chromaffin cell differentiation marker (*Htr3a*) (C34)[28] (Figures 1A–1C, S1C, and S2J). We named this cluster "committed NCC/SCP." C34 forms two branches on the UMAP. The first is composed of cells at E10.5 that express a higher level of *Ret* and connect to early *Slc18a3*^{low}/*Chga*^{low}/*Ret*$^+$ sympathoblasts (C47). The second is composed of adrenal cells at E12.5 that express a higher level of *Hrt3a* and form a continuum with early *Slc18a3*$^-$/*Chga*^{high} and late *Slc18a3*$^-$/*Chga*^{high}/*Foxq1*$^+$ chromaffin cells (C28 and C31, respectively). This is in agreement with the work of Furlan et al.,[28] which revealed unexpected lineage segregation between sympathetic and adrenergic lineages at early stages. Late *Slc18a3*^{high}/*Chga*^{low} sympathoblasts (C41) were obtained from adrenal gland samples at E12.5.

The smallest cluster of our dataset is composed of notochord cells at E9 cells that express the *Noggin*, *Shh*, and *T* genes (C51) (Figures 1A–1C, S1C, and S2I).

Paraxial mesoderm-derived cells are divided into *Meox2*$^+$/*Pax3*$^+$ dermomyotome (C2), *Meox2*$^+$/*Pax9*$^+$ sclerotome (C12 and C19), *Myog*$^+$ myotome (C50), and *Acta2*$^+$ mural cells (C43)[29] (Figures 1C and S2H). An additional *Meox2*$^+$ cell population, negative for dermomyotomal, sclerotomal, or myotomal markers, is present and has been termed "paraxial mesoderm" (C24). All populations derived from the paraxial mesoderm, with the exception of mural cells, were derived from E9 samples (Figures 1A and S1C).

The nephrogenic lineage was identified by *Pax2*$^+$/*Pax8*$^+$ expression and includes E9 IM (C26), *Tfap2b*^{low}/*Calb1*^{high}/*Wnt9b*^{high} caudal and *Tfap2b*^{high}/*Calb1*^{low}/*Wnt9b*^{low} rostral nephric ducts (C33 and C37, respectively),[30] *Cdh1*$^+$/*Jag1*$^+$ mesonephric tubules (C38), and *Cdh1*$^-$ mesonephric/metanephric mesenchyme (C21) (Figures 1A–1C, S1C, and S2G). C21 contains two subgroups of cells with mutually exclusive expression of the nephrogenic mesenchymal markers *Six2*/*Eya1* and mesonephric tubules markers *Lhx1*/*Osr2* (Figure S2G), indicating that both uncommitted and committed tubular progenitors are present in this cluster.

In addition to the nephrogenic structures, the mesonephric ridges contain additional cell populations with, in particular, mesenchymal cells possessing mutually exclusive expression of the stromal markers *Foxd1*/*Cxcl12* and mesonephric mesenchymal markers *Wnt4*/*Gata2*/*Tbx3* (Figures 1C and S1F). The latter group of cells, however, was distinct from *Wnt4*$^+$ mesonephric/metanephric mesenchymal cells (i.e., C21). We therefore classified these populations into the "mesonephros-associated cell types" lineage. This lineage includes the *Wnt4*$^+$ mesenchyme at E11.5 (C4), three clusters composed of *Wnt4*$^+$ and *Foxd1*$^+$ cells of different developmental stages (C0 for E10.5, C8 for E10.5/E11.5, and C1 for E11.5), and CE cells (*Upk3b*$^+$/*Wnt4*$^+$) expressing markers of Müllerian duct progenitors (*Dach2*/*Pax8*) (C13), present as early as E10.5 (Figures 1A, 1C, S1C, and S2F).

The LPM lineage originated from E9 samples and contains *Foxf1*$^+$/*Tbx5*$^-$ splanchnic and *Foxf1*$^-$/*Tbx5*$^+$ somatic compartments (C32 and C39, respectively) (Figures 1A, 1C, and S1C). Overall, our dataset provides a comprehensive overview of the expected adrenogonadal cell types as well as surrounding tissues, present before and during AGP specification, as well as the more differentiated adrenogonadal lineages. This adrenogonadal developmental atlas is freely accessible through an interactive web portal (https://lmedapp731.unige.ch/dataset02/), allowing users to query for genes of interest per cell types, age and sex.

In silico reconstruction of AGP separation refines known and novel marker genes kinetics

To investigate the transcriptional programs underlying AGP specification and fate choice toward adrenal or gonadal identity, we focused our analysis on cells annotated as "coelomic epithelium adrenogonadal primordium" (C7), "coelomic epithelium gonadal primordium" (C17), and "adrenal primordium" (C27). These cells were visualized using a force-directed layout, resulting in a V-shape structure with AGP cells at the base of two branches composed of cells from the gonadal or adrenal primordia reflecting AGP separation (Figure 2A). A refined clustering revealed high heterogeneity and transitional cellular states with 8 subclusters (subC) (Figure 2B). Gene expression analysis together with partition-based graph abstraction (PAGA)[31] defined a common trajectory made of "early AGP" (subC1), "late AGP," and "dividing late AGP" cells (subC6 and subC3, respectively); a gonadal trajectory made of "early" and "late

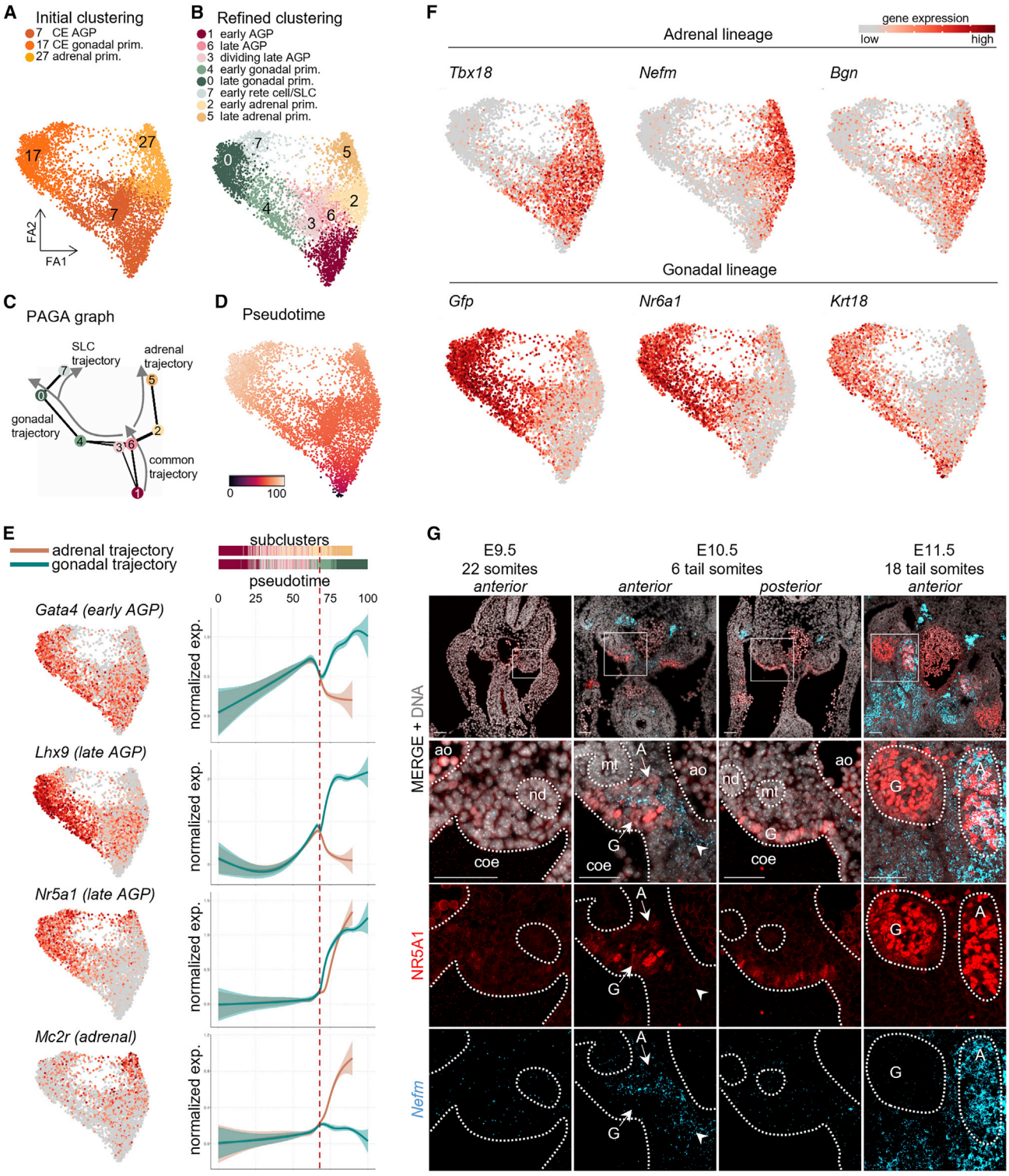

Figure 2. *In silico* reconstruction of adrenogonadal primordium separation refines the kinetics of known and novel marker genes

(A and B) Visualization of the 5,128 transcriptomes in a force-directed layout colored by initial clustering (A) and new refined clustering (B). Cell type annotation is shown on the top. AGP, adrenogonadal primordium; CE, coelomic epithelium; SLC, supporting-like cell.

(C) PAGA representation of the refined clustering. Each node is a cluster, and the edges between clusters represent connectivities. Edges with low connectivities (below 0.3) are not represented. Arrows indicate the common, gonadal, adrenal, and SLC trajectories.

(legend continued on next page)

gonadal primordium'' cells (subC4 and subC0, respectively); and an adrenal trajectory made of ''early'' and ''late adrenal primordium'' cells (subC2 and subC5, respectively) (Figures 2C–2E and S3; Table S2). We have recently shown that rete progenitor cells or ''SLCs'' are specified as early as E10.5 and represent a CE-derived lineage diverging from the gonadal somatic cell lineage.[22] Therefore, the ''early rete cell/SLC'' cluster (subC7), which represents the earliest cells of the SLC lineage, was not taken into account for further analysis. Expression of AGP markers along pseudotime shows that *Gata4/Wt1* detection precedes *Lhx9/Emx2* expression, followed by *Nr5a1* induction (Figures 2E and S3), in accordance with previous reports.[2,3] Shortly after *Nr5a1* detection, these genes adopt gonadal- and adrenal-lineage-specific expression profiles: they are downregulated in cells of the adrenal lineage concomitant with *Mc2r/Nr5a1* upregulation, whereas they are further upregulated in gonadal lineage together with induction of the supporting and steroidogenic cell markers *Gadd45g* and *Cbln1*. Interestingly, the *Nr5a1*$^+$ cellular state preceding lineage diversification (highlighted by a dotted red line in Figures 2E and S3) is composed in majority by cells of subC2 (''early AP'') and subC4 (''early GP'') of the adrenal and gonadal lineages, respectively. This indicates that *Nr5a1* expression is induced in two distinct cell populations. Differential expression analysis between these two subCs (Table S2) provides a set of genes whose expression is specific/enriched in adrenal- or gonadal-committed cells, possibly prior to *Nr5a1* expression. In addition to CE markers (*Myrf*, *Upk3b*, *Krt18*) and early adrenogonadal master genes (*Wt1*, *Lhx9*, *Emx2*, *Amhr2*), gonadal-committed cells express higher amount of *Nr5a1-EGFP* and *Nr6a1*. On the other hand, adrenal-committed cells are characterized by expression of genes encoded for neurofilaments proteins (*Nefm*, *Nefl*), extracellular matrix (*Col25a1*, *Bgn*), and the transcription factor *Tbx18* (Table S2; Figure 2F). RNAScope analysis of the *Nefm* expression profile from E9.5 to E11.5 confirmed that this gene is expressed in *Nr5a1*$^+$ adrenal cells but not in *Nr5a1*$^+$ gonadal cells, as well as in *Nr5a1*$^-$ cells in the vicinity of the AP (E10.5) and the fetal cortex (E11.5) (Figure 2G). Furthermore, the expression profile of *Tbx18* in adrenal-committed cells was confirmed by *in vivo* lineage tracing, revealing not only that this gene is specifically expressed in early adrenal progenitor cells of the anterior CE but that it occurs prior to NR5A1 expression.[32]

Taken together, pseudotime ordering recapitulates the sequential expression kinetics and dynamics of known AGP markers, providing a robust tool to investigate the global transcriptomic signatures associated with each differentiation step. Importantly, it challenges the view of a common *Nr5a1*$^+$ progenitor and suggests that CE cells are already specified toward either adrenal or gonadal fate before delamination and ingression within the underlying mesenchyme.

Adrenal fate choice is associated with inhibition of canonical Wnt signaling and enhanced Rho signaling gene expression

To characterize the transcriptomic programs underlying adrenal versus gonadal cell commitment, we selected 1,737 genes with dynamic expression patterns along pseudotime (see STAR Methods) and grouped them according to their expression similarities. We obtained 22 gene profiles (Ps) (Table S3) including 10 and 7 profiles for which gene expression increased during gonadal and adrenal specification, respectively, and 5 profiles displaying sequential and transitory expression dynamics common to both lineages (Figure S4A). Genes of P16, P13, and P7 are upregulated during gonadal progression. Gene Ontology (GO) analysis (Table S4; Figure S4A) associated these genes with terms such as ''regulation of reproductive process'' (P16; *Sulf1*, *Mafb*), ''positive regulation of gonad development'' (P13; *Wt1*, *Amhr2*), and ''reproductive structure development'' (P7; *Nr0b1*, *Lef1*, *Igf1*, *Lhx9*, *Rspo1*, *Emx2*, *Msx1*, *Lgals7*, *Lgr4*). One profile contains gonadal-specific CE genes (P20; *Upk3b*, *Myrf*), together with genes coding for keratins, indicating that CE maturation accompanies gonadal specification.

Regarding adrenal enriched programs, genes of P4, P8, P17, P1, and P2 are expressed in both lineages prior to adrenal or gonadal specification and are progressively downregulated in gonadal cells, whereas expression is maintained or further increased in adrenal cells. GO analysis associated these genes with ''cell-cell signaling by Wnt,'' ''Wnt signaling pathway PCP pathway,'' and ''regulation of WNT signaling pathway.'' Genes belonging to these terms (*Sfrp1*, *Sfrp2*, *Nkd1*, *Sox9*, *Dact1*, *Fzd1*, *Hmga2*, *Shisa3*, *Ror1*, *Daam2*, *Nfatc4*, *Vgll4*; Table S4; Figures 3A and S4A) are all annotated as ''negative regulation of canonical Wnt signaling pathway'' in the GO database. In line with their opposite expression levels between adrenal and gonadal lineages, the target of the canonical Wnt signaling *Lef1* (P7) is induced in gonadal, but not adrenal, cells both at the transcriptomic (Figure 3A) and protein (Figure 3B) levels. Adrenal programs involve genes associated with ''Rho protein signal transduction'' (P17), ''regulation of actin filament-based process'' (P17), ''positive regulation of cytoskeleton organization'' (P10), ''extracellular matrix organization'' (P4 and P8), and ''collagen metabolic process'' (P1) (Table S4; Figure S4B), suggesting that non-canonical Wnt activation of Rho signaling is at play in AGP and AP cells to positively modulate cell movement and interaction with extracellular matrix. This is consistent with the morphogenetic events taking place in the AGP, as cells delaminate from the CE and undergo an epithelial-to-mesenchymal transition (EMT). Accordingly, the EMT inducers *Twist1*, *Zeb2*, and *Foxc1*[33] are regulated in a similar manner (P8).

(D) Visualization of the transcriptomes colored by pseudotime.
(E) Expression levels of representative known marker genes in a force-directed layout (left) and along pseudotime (right, y axis: normalized expression, x axis: pseudotime). The vertical dotted red line indicates an *Nr5a1*$^+$ cellular state preceding lineage diversification.
(F) Expression levels of novel marker genes of adrenal (top) and gonadal (bottom) specifications in a force-directed layout.
(G) Co-labeling for NR5A1 (immunostaining) and *Nefm* mRNA (RNAScope *in situ* hybridization) in E9.5, E10.5, and E11.5 embryos (transverse sections), revealing overlapping expression profiles in adrenal progenitors. Arrows point to NR5A1$^+$ gonadal and adrenal fields, while the arrowhead points to *Nefm*$^+$ cells devoid of NR5A1 expression. A, adrenal field, ao, aorta; coe, coelomic cavity; G, gonadal field; mt, mesonephric tubule; nd, nephric duct. Scale bars, 50 μm.

CellPress
OPEN ACCESS

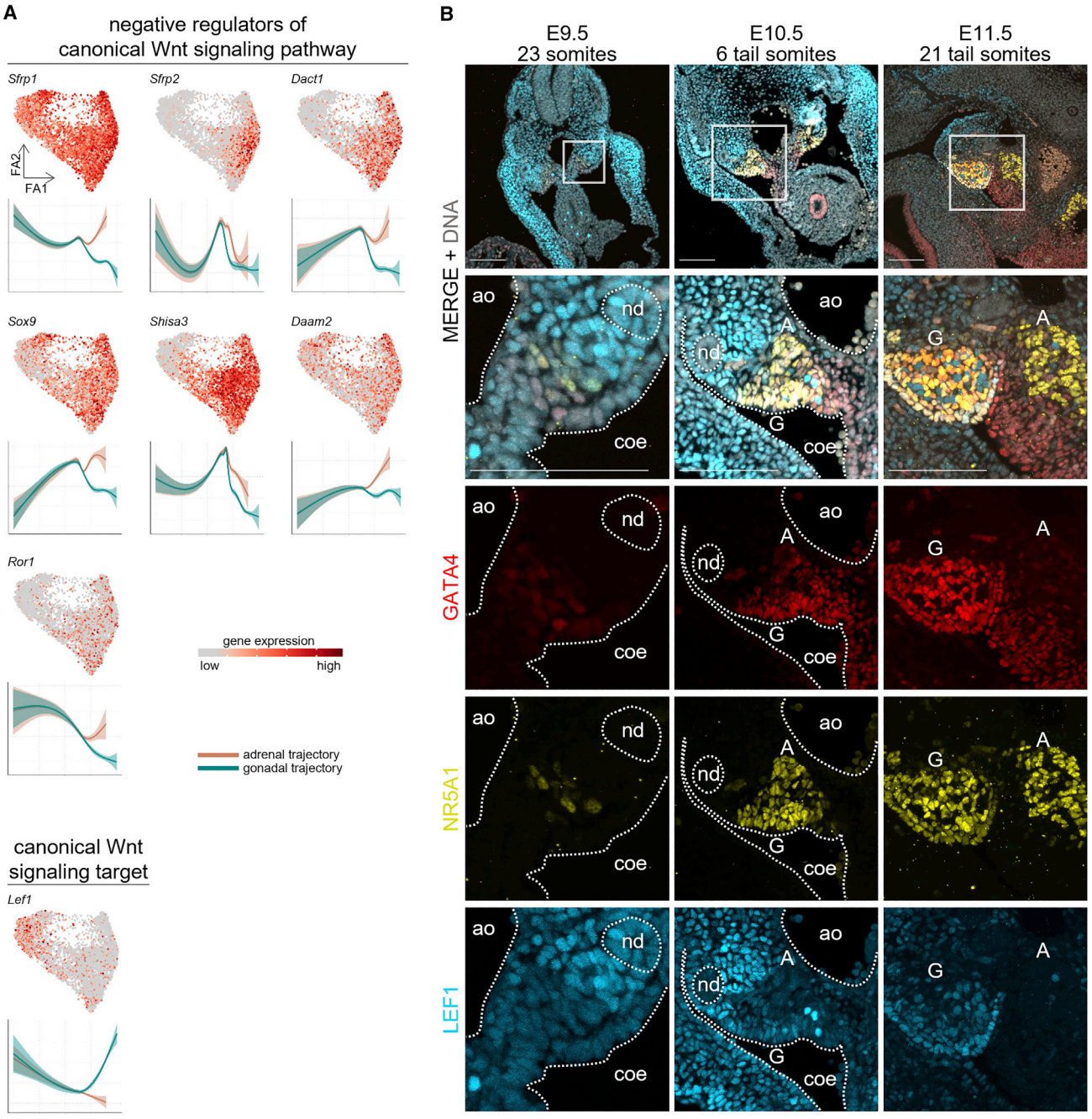

Figure 3. Adrenal fate choice is associated with inhibition of canonical Wnt signaling

(A) Expression levels of negative regulators and target of the canonical Wnt signaling in a force-directed layout (top) and along pseudotime (bottom, y axis: normalized expression, x axis: pseudotime) showing opposite expression levels along adrenal and gonadal trajectories.

(B) Co-labeling for GATA4, NR5A1, and LEF1 (immunostaining) in E9.5, E10.5, and E11.5 embryos (transverse sections), revealing LEF1 expression in gonadal, but not adrenal, progenitors. A, adrenal field, ao, aorta; coe, coelomic cavity; G, gonadal field; nd, nephric duct. Scale bars, 100 μm.

Early AGP gene signatures indicate a LPM origin and dynamic *Hox* expression programs

To get insights into the gene programs underlying early AGP cell specification prior to *Nr5a1* expression, we focused on the gene profiles displaying high expression at the start of the pseudotime. Among the 22 profiles, P14 included genes that have early and robust high expression levels and are rapidly downregulated as the cells progress to the late AGP state (Figure S4A). These genes are associated with the GO term "cardiac right ventricle morphogenesis," including *Isl1*, *Hand1*, *Hand2*, and *Gata3,* which are known markers of the proepicardium, a CE-derived structure (Figure S4C). P14 also includes *Hlx* expressed in the

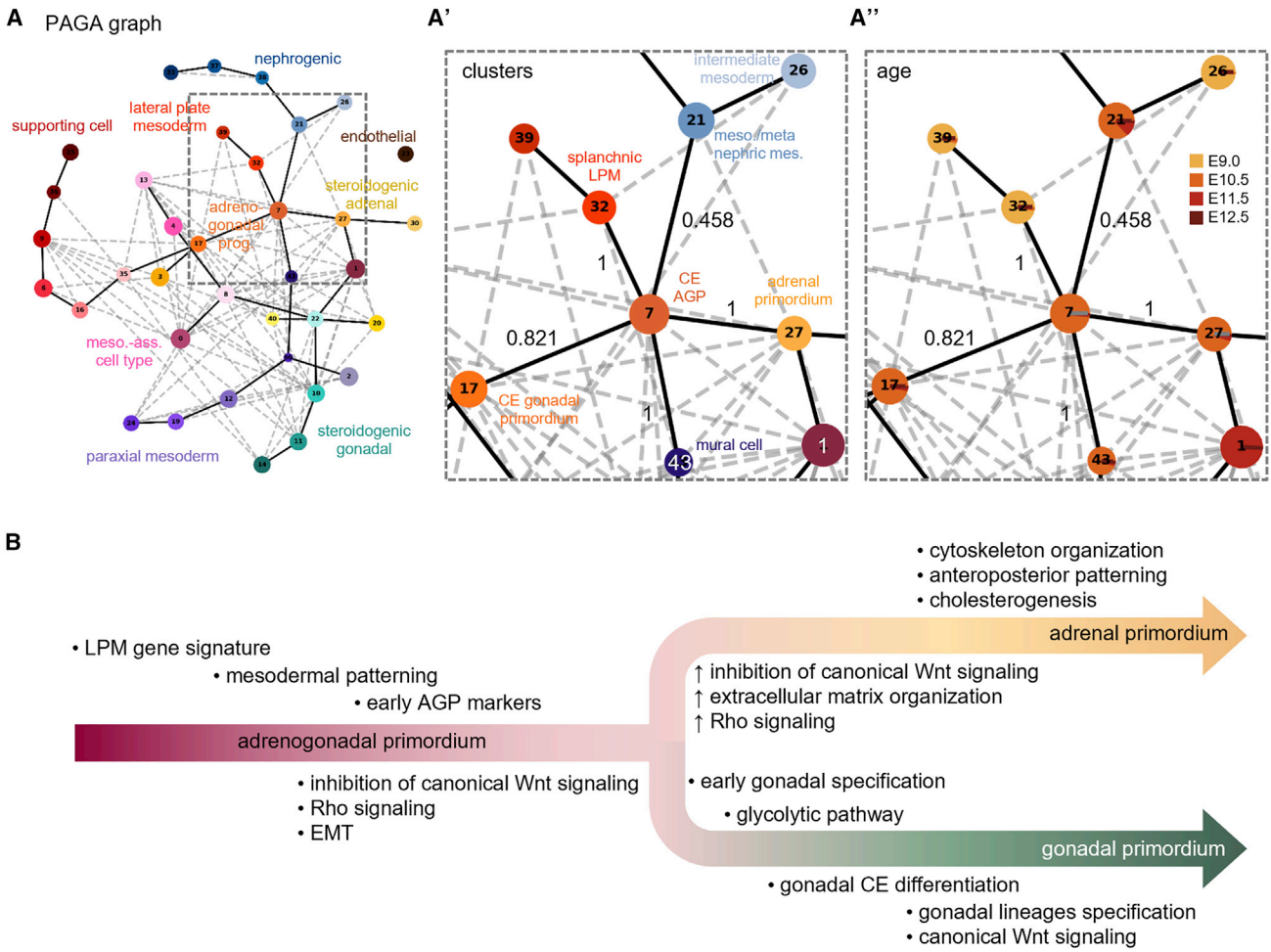

Figure 4. Lineage reconstruction of mesodermal-derived cell types from E9 to E12.5

(A) PAGA representation of the mesodermal-derived cell clusters from Figure 1B. Each node is a cluster, and the edges between clusters represent connectivities. Edges with low connectivities (below 0.25) are not represented. Major lineages are indicated. The inset shows the connectivity scores (black numbers) of cluster 7 (CE AGP) with clusters 17, 21, 27, 32, and 43 and are colored by clustering (A′) and by age (A″).

(B) Model of cell lineage specification during adrenogonadal primordium separation. AGP, adrenogonadal primordium; CE, coelomic epithelium; LPM, lateral plate mesoderm;; meso.-ass., mesonephros-associated; meso./metanephric mes., mesonephric/metanephric mesenchyme.

septum transversum.[34] The finding that the early AGP gene signature reflects that found in proepicardium/septum transversum cells, which are derived from the LPM,[35] suggests that the AGP also originates from the LPM rather than the IM. To confirm this hypothesis, we compared the PAGA connectivity's scores, indicating potential ontogenic relationships, among mesodermal-derived cell types of our whole dataset (E9–E12.5). Indeed, this analysis showed that AGP cells (C7 of our initial clustering) are transcriptionally closer to splanchnic LPM at E9 (C39) than IM at E9 and meso/metanephric mesenchymal cells at E10.5 (C26 and C21, respectively) (Figure 4A).

The other profiles with high gene expression in early AGP cells include P12 and P3, which are downregulated during both adrenal and gonadal cell specification, and P4, P8, and P17, which are downregulated in the gonadal lineage only (Figure S4A). GO annotations common to these profiles include "proximal/distal pattern formation" and "pattern specification process," with corresponding genes including several *Hox* genes (P3 and 17) and mesodermal markers such as *Nr2f1*, *Nr2f2*, *Meis1–3*, *Pitx2*, and *Gli3* (P8 and P17). *Hox* genes encode transcriptional regulatory proteins and are organized in four genomic clusters (*Hoxa*, *-b*, *-c*, and *-d*) expressed from 3′ to 5′ along the anteroposterior body plan.[36] Interestingly, *Hoxa9-10*, *Hoxc9-10*, and *Hoxd10* genes are downregulated in both lineages (P3), while the expression of *Hoxa2*, *-3*, *-5*, and *-7* genes is maintained in adrenal cells (P17). In addition, *Hoxb2–9* and *Hoxc4–6* expression increased as cells adopt an adrenal fate (P10) (Figure S4D). Several *Hox* genes have been shown to be abundantly expressed in AP cells, where they directly bind and positively regulate *Nr5a1* expression.[37] Since our analysis shows differential expression of the *Hox* genes along adrenal and gonadal fate commitment, and since the AP is specified in the more anterior region of the genital ridge, it is possible that specific sets of *Hox* genes determine adrenal versus gonadal fate choice.

DISCUSSION

Although adrenogonadal development has been studied for several decades, the composition and molecular signatures of early adrenogonadal progenitors is still incomplete. In addition, the genetic programs and regulatory factors orchestrating the separation of the AGP into two distinct primordia remain poorly characterized. Here, we generated a comprehensive single-cell transcriptomic atlas of mouse adrenogonadal cells and surrounding tissues collected before, during, and after AGP separation without prior selection of cells by lineage markers. This detailed atlas comprising 52 cell types represents a valuable resource that is freely available to the scientific community in an interactive website (https://lmedapp731.unige.ch/dataset02/).

Using this atlas, we showed that the AGP and the gonadal and adrenal primordia at E10.5 display distinct transcriptomic identities. Lineage reconstruction and pseudotime analysis allowed us to uncover the dynamic genetic programs at play during AGP cell specification toward the adrenal or gonadal fate, unraveling differential cellular processes underlying this fate choice (model depicted in Figure 4B). We found that the canonical Wnt pathway is actively repressed in uncommitted AGP cells, and this repression is maintained or further increased as the cells progress through the adrenal lineage. In contrast, cells adopting a gonadal fate release this inhibition and activate the canonical Wnt pathway required for their proliferation.[38] On the other hand, cells of the AGP and the adrenal primordia appear to activate the planar cell polarity pathway as they undergo Rho signaling-dependent rearrangement of actin filament and cytoskeleton, concomitant with active interaction with extracellular matrix components and the EMT. These processes may be important for the cells with adrenal fate to move to a more dorso-medial position than the gonadal ridge, allowing proper positioning of the future fetal cortex within the urogenital tract. Indeed, between E11.5 and E14.5, the fetal adrenal undergoes extensive morphogenetic events, such as invasion by SCPs to form the adrenal medulla and encapsulation by surrounding mesenchymal cells to form the adult adrenal cortex.[6] Furthermore, the dorso-medial positioning of the fetal cortex may be important to reach an "adrenal niche" presenting optimal cues from surrounding tissues for proper differentiation into fetal adrenal steroidogenic cells. Interestingly, mice mutant for *Wnt4*, a gene that has been reported to induce non-canonical Wnt signaling in several organs,[39–41] exhibit mislocalization of adrenal cells at the anterior pole of the gonads,[42–44] supporting our model that non-canonical, adrenal-specific Wnt signaling allows for proper separation of the gonadal and adrenal primordia. At later stages, adrenal development does, however, rely on β-catenin,[45] suggesting that specification and growth are governed by distinct mechanisms. Considering the differential combinations of *Hox* genes expressed in cells destined to become adrenal and gonadal cells, it appears that the specification/separation of adrenal and gonadal primordia involves a complex integration of positional information as well as dedicated cellular processes allowing proper patterning of adrenogonadal ridges. Indeed, anterior *Hox* paralog expression is higher in early adrenal progenitors compared with early gonadal progenitors (Figures S5D and S5E). This includes *Hoxa2*, *Hoxb5*, and *Hoxc5-6* (Figure S4), which have been shown to bind the fetal adrenal enhancer (FAdE) of *Nr5a1*,[37] targeting expression in the AP but not in the GP. The expression of *Hox* paralogs is under the control of retinoic acid signaling,[46] a well-known morphogen required for anteriorization of the mesoderm. Taken together, it is likely that retinoic acid signaling, through the activation of members of the *Hox* gene cluster, induces *Nr5a1* expression in the more rostrally located adrenal progenitors.

Our findings are consistent with a recent study in humans and cynomolgus monkeys, which revealed that both the adrenocortical and gonadal cell lineages originate in the CE but in a spatially and temporally distinct manner.[47] In humans, the adrenocortical lineage is specified early in the anterior part of the CE, while the gonadal lineage appears later in the posterior part of the CE. Similarly, in the mouse, the AP is specified in the most anterior region of the genital ridge. In both mice and humans, the adrenocortical and gonadal lineages have different expression profiles of *HOX/Hox* genes (see Figure S4D and Cheng et al.[47]). This suggests that the spatially expressed HOX gene set confers regional identity along the anterior-posterior axis, allowing the establishment of specific transcriptional programs that direct adrenal or gonadal cell fates. Therefore, distinct specification of these two lineages appears to be evolutionary conserved between both mouse and human.

Careful analysis of the expression profile of the known early adrenogonadal markers along pseudotime revealed that *Nr5a1* is expressed relatively late within the AGP differentiation window, a time point when cells are already committed toward the gonadal or the adrenal fate. This reveals that the use of *Nr5a1* as a marker of the CE to define a common AGP is incorrect and raises the question of whether CE cells are already specified toward a given fate before delamination and ingression within the underlying mesenchyme. Among others, we identified the gene encoding the neurofilament protein *Nefm* and the transcription factor *Tbx18* to be expressed prior to *Nr5a1* in the adrenal lineage. *Nefm* expression was absent in the urogenital ridge at E9.5 but could be detected in the rostral—but not caudal—urogenital tract at E10.5. Of note, all *Nefm*$^+$ cells expressing NR5A1 were found in the adrenal but not the gonad. Also consistent with our findings, *Tbx18* has been shown previously to be expressed in the anterior CE as early as E9.5 and this was specifically in early adrenal progenitors, even before NR5A1 expression.[32]

The origin of early adrenogonadal cells is disputed, as it remains unclear whether they are derived from the lateral plate or the IM. Indeed, the only cell lineage-tracing studies of CE cells in mouse were performed after AGP separation.[10,11] We used our single-cell dataset comprising cells from all three layers of mesodermal derivatives (paraxial, lateral, and intermediate) present at E9 in the posterior trunk to show that in mouse, early AGP cells are ontogenically related to the splanchnic LPM. The relevance of different origins for the AGP among vertebrates—LPM in mouse (this study) and IM in chicken[7–9]—is not clear, but it has been proposed to be linked to differences in mesonephros excretory function and/or evolution of master sex-determining genes.[48] Interestingly, we observed discrepancies between *Nr5a1-EGFP* transgene and endogenous *Nr5a1* expression, with *GFP* being expressed in a subset of *Pax2*$^+$/*Nr5a1*$^-$ IM at E9 (Figures S5A–S5C). Given that the *Nr5a1-EGFP* transgene and the endogenous *Nr5a1* locus differ in their regulatory regions (for comparison, see Stallings et al.[14] and Zubair et al.[37]), the observed induction of *Nr5a1-EGFP* in mouse IM

could reflect an ancestral adrenogonadal fate specification competence that has been switched off during evolution. Comparative mouse and chicken mesodermal single-cell transcriptomic and epigenomic profiling could provide insights into the evolutionary divergence of regulatory processes of adrenogonadal specification. In chicken embryo, for example, SHH and BMP4 play a central role in the initiation of gonadal differentiation.[49] However, comparative expression analysis calls into question the requirement of Hedgehog and BMP4 signaling for gonadal differentiation in mice. Indeed, according to our single-cell expression data atlas (Figure S2I; data not shown), the expression profiles are different in the mouse. Moreover, it was shown that SHH signaling is not required for both gonad specification and AP formation in the mouse.[24,50,51]

In summary, the comprehensive atlas of adrenogonadal development described here allowed us to determine the precise origin of the adrenal cortex and gonads in the mouse. Our findings that development of these two organs diverges before the induction of *Nr5a1* indicates that this gene should no longer be used as a marker for the common primordium.

Limitations of the study

An important part of our conclusions is based on bioinformatic analyses of single-cell expression data. Due to technical difficulties and the absence of suitable Cre lines, it is presently difficult to independently confirm all conclusions *in vivo*. Indeed, to our knowledge, there is no mouse model allowing us to follow, by lineage tracing, the fate of AP and GP progenitors. Moreover, RNAscope analyses are not always successful either because the expression of marker genes is low and/or because RNAscope probes do not work efficiently. These technical limitations prevent us, for example, to demonstrate *in vivo* that the AP and the GP are specified prior to *Nr5a1* expression.

STAR★METHODS

Detailed methods are provided in the online version of this paper and include the following:

- KEY RESOURCES TABLE
- RESOURCE AVAILABILITY
  - Lead contact
  - Materials availability
  - Data and code availability
- EXPERIMENTAL MODEL AND SUBJECT DETAILS
- METHODS DETAILS
  - Single cell suspension and library preparation
  - Sequencing
  - Immunofluorescence and RNAscope analyses
- QUANTIFICATION AND STATISTICAL ANALYSIS
  - Single-cell RNA sequencing analysis
  - Transcriptomic atlas annotation
- ADDITIONAL RESOURCES

SUPPLEMENTAL INFORMATION

Supplemental information can be found online at https://doi.org/10.1016/j.celrep.2023.112191.

ACKNOWLEDGMENTS

We thank the teams of the Flow Cytometry Facility (Faculty of Medicine, University of Geneva); the Animal Facility (Faculty of Medicine, University of Geneva); the DNA Sequencing Platform (Health 2030 Genome Center, Geneva); Dr. Christelle Borel (GEDEV Department, University of Geneva) for help with the 10X Chromium technology; and Dr. Marie-Christine Chaboissier for LEF1 antibody. This work was supported by the Fondation pour la Recherche Médicale (grant number ARF201909009270 to Y.N.); the Swiss National Science Foundation (grant numbers 31003A_173070 and 310030_200316 to S.N.); the Département de l'Instruction Publique of the State of Geneva (to S.N. and Y.N.); La Ligue Contre le Cancer (Equipe Labelisée to A.S.); IFCAH (2022); DFG (CRC/TRR205); and the ANR (ANR-11-LABX-0028-01 and ANR-18-CE14-0012 to A.S.).

AUTHOR CONTRIBUTIONS

Conceptualization, Y.N., S.N., and A.S.; methodology, Y.N. and P.S.; software, P.S. and C.M.; formal analysis and investigation, Y.N., P.S., F.K., C.M., L.C.W.A., and V.R.; resources, S.N.; data curation, Y.N., P.S., and C.M.; writing – original draft, Y.N.; writing – review & editing, Y.N., P.S., S.N., and A.S.; supervision, Y.N., S.N., and A.S.; funding acquisition, Y.N., S.N., and A.S.

DECLARATION OF INTERESTS

The authors declare no competing interests.

INCLUSION AND DIVERSITY

We support inclusive, diverse, and equitable conduct of research.

Received: May 6, 2022
Revised: December 13, 2022
Accepted: February 14, 2023
Published: March 1, 2023

REFERENCES

1. Ikeda, Y., Shen, W.H., Ingraham, H.A., and Parker, K.L. (1994). Developmental expression of mouse steroidogenic factor-1, an essential regulator of the steroid hydroxylases. Mol. Endocrinol. *8*, 654–662. https://doi.org/10.1210/mend.8.5.8058073.
2. Wilhelm, D., and Englert, C. (2002). The Wilms tumor suppressor WT1 regulates early gonad development by activation of Sf1. Genes Dev. *16*, 1839–1851. https://doi.org/10.1101/GAD.220102.
3. Hu, Y.C., Okumura, L.M., and Page, D.C. (2013). Gata4 is required for formation of the genital ridge in mice. PLoS Genet. *9*, e1003629. https://doi.org/10.1371/journal.pgen.1003629.
4. Hatano, O., Takakusu, A., Nomura, M., and Morohashi, K. (1996). Identical origin of adrenal cortex and gonad revealed by expression profiles of Ad4BP/SF-1. Gene Cell. *1*, 663–671. https://doi.org/10.1046/j.1365-2443.1996.00254.x.
5. Bandiera, R., Vidal, V.P.I., Motamedi, F.J., Clarkson, M., Sahut-Barnola, I., von Gise, A., Pu, W.T., Hohenstein, P., Martinez, A., and Schedl, A. (2013). WT1 maintains adrenal-gonadal primordium identity and marks a population of AGP-like progenitors within the adrenal gland. Dev. Cell *27*, 5–18. https://doi.org/10.1016/j.devcel.2013.09.003.
6. Bandiera, R., Sacco, S., Vidal, V.P.I., Chaboissier, M.-C., and Schedl, A. (2015). Steroidogenic organ development and homeostasis: a WT1-centric view. Mol. Cell. Endocrinol. *408*, 145–155. https://doi.org/10.1016/j.mce.2015.01.009.
7. Sekido, R., and Lovell-Badge, R. (2007). Mechanisms of gonadal morphogenesis are not conserved between chick and mouse. Dev. Biol. *302*, 132–142. https://doi.org/10.1016/j.ydbio.2006.09.007.
8. Yoshioka, H., Ishimaru, Y., Sugiyama, N., Tsunekawa, N., Noce, T., Kasahara, M., and Morohashi, K.I. (2005). Mesonephric FGF signaling is

associated with the development of sexually indifferent gonadal primordium in chick embryos. Dev. Biol. *280*, 150–161. https://doi.org/10.1016/J.YDBIO.2005.01.011.

9. Estermann, M.A., Williams, S., Hirst, C.E., Roly, Z.Y., Serralbo, O., Adhikari, D., Powell, D., Major, A.T., and Smith, C.A. (2020). Insights into gonadal sex differentiation provided by single-cell transcriptomics in the chicken embryo. Cell Rep. *31*, 107491. https://doi.org/10.1016/j.celrep.2020.03.055.
10. Karl, J., and Capel, B. (1998). Sertoli cells of the mouse testis originate from the coelomic epithelium. Dev. Biol. *203*, 323–333. https://doi.org/10.1006/dbio.1998.9068.
11. DeFalco, T., Takahashi, S., and Capel, B. (2011). Two distinct origins for Leydig cell progenitors in the fetal testis. Dev. Biol. *352*, 14–26. https://doi.org/10.1016/j.ydbio.2011.01.011.
12. Sasaki, K., Oguchi, A., Cheng, K., Murakawa, Y., Okamoto, I., Ohta, H., Yabuta, Y., Iwatani, C., Tsuchiya, H., Yamamoto, T., et al. (2021). The embryonic ontogeny of the gonadal somatic cells in mice and monkeys. Cell Rep. *35*, 109075. https://doi.org/10.1016/j.celrep.2021.109075.
13. Bullejos, M., and Koopman, P. (2001). Spatially dynamic expression of Sry in mouse genital ridges. Dev. Dynam. *221*, 201–205. https://doi.org/10.1002/dvdy.1134.
14. Stallings, N.R., Hanley, N.A., Majdic, G., Zhao, L., Bakke, M., and Parker, K.L. (2002). Development of a transgenic green fluorescent protein lineage marker for steroidogenic factor 1. Mol. Endocrinol. *16*, 2360–2370. https://doi.org/10.1210/me.2002-0003.
15. Becht, E., McInnes, L., Healy, J., Dutertre, C.A., Kwok, I.W.H., Ng, L.G., Ginhoux, F., and Newell, E.W. (2018). Dimensionality reduction for visualizing single-cell data using UMAP. Nat. Biotechnol. *37*, 38–44. https://doi.org/10.1038/nbt.4314.
16. Rudat, C., Grieskamp, T., Röhr, C., Airik, R., Wrede, C., Hegermann, J., Herrmann, B.G., Schuster-Gossler, K., and Kispert, A. (2014). Upk3b is dispensable for development and integrity of urothelium and mesothelium. PLoS One *9*, e112112. https://doi.org/10.1371/journal.pone.0112112.
17. Hamanaka, K., Takata, A., Uchiyama, Y., Miyatake, S., Miyake, N., Mitsuhashi, S., Iwama, K., Fujita, A., Imagawa, E., Alkanaq, A.N., et al. (2019). MYRF haploinsufficiency causes 46,XY and 46,XX disorders of sex development: bioinformatics consideration. Hum. Mol. Genet. *28*, 2319–2329. https://doi.org/10.1093/hmg/ddz066.
18. Birk, O.S., Casiano, D.E., Wassif, C.A., Cogliati, T., Zhao, L., Zhao, Y., Grinberg, A., Huang, S., Kreidberg, J.A., Parker, K.L., et al. (2000). The LIM homeobox gene Lhx9 is essential for mouse gonad formation. Nature *403*, 909–913. https://doi.org/10.1038/35002622.
19. Niu, W., and Spradling, A.C. (2020). Two distinct pathways of pregranulosa cell differentiation support follicle formation in the mouse ovary. Proc. Natl. Acad. Sci. USA *117*, 20015–20026. https://doi.org/10.1073/PNAS.2005570117.
20. Kulibin, A.Y., and Malolina, E.A. (2020). Formation of the rete testis during mouse embryonic development. Dev. Dynam. *249*, 1486–1499. https://doi.org/10.1002/dvdy.242.
21. Omotehara, T., Wu, X., Kuramasu, M., and Itoh, M. (2020). Connection between seminiferous tubules and epididymal duct is originally induced before sex differentiation in a sex-independent manner. Dev. Dynam. *249*, 754–764. https://doi.org/10.1002/dvdy.155.
22. Mayère, C., Regard, V., Perea-Gomez, A., Bunce, C., Neirijnck, Y., Djari, C., Sararols, P., Reeves, R., Greenaway, S., Simon, M., et al. (2021). Origin, specification and differentiation of a rare supporting-like lineage in the developing mouse gonad. Preprint at bioRxiv. https://doi.org/10.1101/2021.09.15.460431.
23. Miyabayashi, K., Katoh-Fukui, Y., Ogawa, H., Baba, T., Shima, Y., Sugiyama, N., Kitamura, K., and Morohashi, K.i. (2013). Aristaless related homeobox gene, Arx, is implicated in mouse fetal Leydig cell differentiation possibly through expressing in the progenitor cells. PLoS One *8*, e68050. https://doi.org/10.1371/journal.pone.0068050.
24. King, P., Paul, A., and Laufer, E. (2009). Shh signaling regulates adrenocortical development and identifies progenitors of steroidogenic lineages. Proc. Natl. Acad. Sci. USA *106*, 21185–21190. https://doi.org/10.1073/PNAS.0909471106.
25. Wood, M.A., Acharya, A., Finco, I., Swonger, J.M., Elston, M.J., Tallquist, M.D., and Hammer, G.D. (2013). Fetal adrenal capsular cells serve as progenitor cells for steroidogenic and stromal adrenocortical cell lineages in M. musculus. Development *140*, 4522–4532. https://doi.org/10.1242/DEV.092775.
26. Zubair, M., Parker, K.L., and Morohashi, K.i. (2008). Developmental links between the fetal and adult zones of the adrenal cortex revealed by lineage tracing. Mol. Cell Biol. *28*, 7030–7040. https://doi.org/10.1128/MCB.00900-08.
27. Mayère, C., Neirijnck, Y., Sararols, P., Rands, C.M., Stévant, I., Kühne, F., Chassot, A.A., Chaboissier, M.C., Dermitzakis, E.T., and Nef, S. (2021). Single-cell transcriptomics reveal temporal dynamics of critical regulators of germ cell fate during mouse sex determination. FASEB J. *35*, 21452. https://doi.org/10.1096/fj.202002420R.
28. Furlan, A., Dyachuk, V., Kastriti, M.E., Calvo-Enrique, L., Abdo, H., Hadjab, S., Chontorotzea, T., Akkuratova, N., Usoskin, D., Kamenev, D., et al. (2017). Multipotent peripheral glial cells generate neuroendocrine cells of the adrenal medulla. Science *357*, eaal3753. https://doi.org/10.1126/science.aal3753.
29. Wasteson, P., Johansson, B.R., Jukkola, T., Breuer, S., Akyürek, L.M., Partanen, J., and Lindahl, P. (2008). Developmental origin of smooth muscle cells in the descending aorta in mice. Development *135*, 1823–1832. https://doi.org/10.1242/DEV.020958.
30. Sanchez-Ferras, O., Pacis, A., Sotiropoulou, M., Zhang, Y., Wang, Y.C., Bourgey, M., Bourque, G., Ragoussis, J., and Bouchard, M. (2021). A coordinated progression of progenitor cell states initiates urinary tract development. Nat. Commun. *12*, 2627–2716. https://doi.org/10.1038/s41467-021-22931-5.
31. Wolf, F.A., Hamey, F.K., Plass, M., Solana, J., Dahlin, J.S., Göttgens, B., Rajewsky, N., Simon, L., and Theis, F.J. (2019). PAGA: graph abstraction reconciles clustering with trajectory inference through a topology preserving map of single cells. Genome Biol. *20*, 59. https://doi.org/10.1186/S13059-019-1663-X.
32. Häfner, R., Bohnenpoll, T., Rudat, C., Schultheiss, T.M., and Kispert, A. (2015). Fgfr2 is required for the expansion of the early adrenocortical primordium. Mol. Cell. Endocrinol. *413*, 168–177. https://doi.org/10.1016/j.mce.2015.06.022.
33. Meyer-Schaller, N., Cardner, M., Diepenbruck, M., Saxena, M., Tiede, S., Lüönd, F., Ivanek, R., Beerenwinkel, N., and Christofori, G. (2019). A hierarchical regulatory landscape during the multiple stages of EMT. Dev. Cell *48*, 539–553.e6. https://doi.org/10.1016/J.DEVCEL.2018.12.023.
34. Lints, T.J., Hartley, L., Parsons, L.M., and Harvey, R.P. (1996). Mesoderm-specific expression of the divergent homeobox gene HZx during murine embryogenesis. Dev. Dynam. *205*, 457–470. https://doi.org/10.1002/(SICI)1097-0177(199604)205:4<457::AID-AJA9>3.0.CO;2-H.
35. Cano, E., Carmona, R., Ruiz-Villalba, A., Rojas, A., Chau, Y.Y., Wagner, K.D., Wagner, N., Hastie, N.D., Muñoz-Chápuli, R., and Pérez-Pomares, J.M. (2016). Extracardiac septum transversum/proepicardial endothelial cells pattern embryonic coronary arterio-venous connections. Proc. Natl. Acad. Sci. USA. *113*, 656–661. https://doi.org/10.1073/PNAS.1509834113/SUPPL_FILE/PNAS.1509834113.SM04.AVI.
36. Deschamps, J., and Duboule, D. (2017). Embryonic timing, axial stem cells, chromatin dynamics, and the Hox clock. Genes & development *31*, 1406–1416. https://doi.org/10.1101/gad.303123.
37. Zubair, M., Ishihara, S., Oka, S., Okumura, K., and Morohashi, K.i. (2006). Two-step regulation of Ad4BP/SF-1 gene transcription during fetal adrenal development: initiation by a Hox-Pbx1-Prep1 complex and maintenance via autoregulation by Ad4BP/SF-1. Mol. Cell Biol. *26*, 4111–4121. https://doi.org/10.1128/MCB.00222-06.
38. Chassot, A.A., Bradford, S.T., Auguste, A., Gregoire, E.P., Pailhoux, E., de Rooij, D.G., Schedl, A., and Chaboissier, M.C. (2012). WNT4 and RSPO1 together are required for cell proliferation in the early mouse gonad. Development *139*, 4461–4472. https://doi.org/10.1242/DEV.078972.
39. Eliazer, S., Muncie, J.M., Christensen, J., Sun, X., D'Urso, R.S., Weaver, V.M., and Brack, A.S. (2019). Wnt4 from the niche controls the

mechano-properties and quiescent state of muscle stem cells. Cell Stem Cell *25*, 654–665.e4. https://doi.org/10.1016/j.stem.2019.08.007.

40. Louis, I., Heinonen, K.M., Chagraoui, J., Vainio, S., Sauvageau, G., and Perreault, C. (2008). The signaling protein Wnt4 enhances thymopoiesis and expands multipotent hematopoietic progenitors through β-catenin-independent signaling. Immunity *29*, 57–67. https://doi.org/10.1016/j.immuni.2008.04.023.
41. Tanigawa, S., Wang, H., Yang, Y., Sharma, N., Tarasova, N., Ajima, R., Yamaguchi, T.P., Rodriguez, L.G., and Perantoni, A.O. (2011). Wnt4 induces nephronic tubules in metanephric mesenchyme by a non-canonical mechanism. Dev. Biol. *352*, 58–69. https://doi.org/10.1016/j.ydbio.2011.01.012.
42. Heikkilä, M., Peltoketo, H., Leppäluoto, J., Ilves, M., Vuolteenaho, O., and Vainio, S. (2002). Wnt-4 deficiency alters mouse adrenal cortex function, reducing aldosterone production. Endocrinology *143*, 4358–4365. https://doi.org/10.1210/en.2002-220275.
43. Jeays-Ward, K., Hoyle, C., Brennan, J., Dandonneau, M., Alldus, G., Capel, B., and Swain, A. (2003). Endothelial and steroidogenic cell migration are regulated by WNT4 in the developing mammalian gonad. Development *130*, 3663–3670. https://doi.org/10.1242/DEV.00591.
44. Val, P., Jeays-Ward, K., and Swain, A. (2006). Identification of a novel population of adrenal-like cells in the mammalian testis. Dev. Biol. *299*, 250–256. https://doi.org/10.1016/J.YDBIO.2006.07.030.
45. Kim, A.C., Reuter, A.L., Zubair, M., Else, T., Serecky, K., Bingham, N.C., Lavery, G.G., Parker, K.L., and Hammer, G.D. (2008). Targeted disruption β-catenin in Sf1-expressing cells impairs development and maintenance of the adrenal cortex. Development *135*, 2593–2602. https://doi.org/10.1242/dev.021493.
46. Nolte, C., De Kumar, B., and Krumlauf, R. (2019). Hox genes: downstream "effectors" of retinoic acid signaling in vertebrate embryogenesis. Genesis *57*, e23306. https://doi.org/10.1002/dvg.23306.
47. Cheng, K., Seita, Y., Moriwaki, T., Noshiro, K., Sakata, Y., Hwang, Y.S., Torigoe, T., Saitou, M., Tsuchiya, H., Iwatani, C., et al. (2022). The developmental origin and the specification of the adrenal cortex in humans and cynomolgus monkeys. Sci. Adv. *8*, eabn8485.
48. Estermann, M.A., Major, A.T., and Smith, C.A. (2020). Gonadal sex differentiation: supporting versus steroidogenic cell lineage specification in mammals and birds. Front. Cell Dev. Biol. *8*, 616387–616410. https://doi.org/10.3389/fcell.2020.616387.
49. Yoshino, T., Murai, H., and Saito, D. (2016). Hedgehog-BMP signalling establishes dorsoventral patterning in lateral plate mesoderm to trigger gonadogenesis in chicken embryos. Nat. Commun. *7*, 12561. https://doi.org/10.1038/ncomms12561.
50. Murashima, A., Akita, H., Okazawa, M., Kishigami, S., Nakagata, N., Nishinakamura, R., and Yamada, G. (2014). Midline-derived Shh regulates mesonephric tubule formation through the paraxial mesoderm. Dev. Biol. *386*, 216–226. https://doi.org/10.1016/j.ydbio.2013.12.026.
51. Hu, M.C., Mo, R., Bhella, S., Wilson, C.W., Chuang, P.T., Hui, C.C., and Rosenblum, N.D. (2006). GLI3-dependent transcriptional repression of Gli1, Gli2 and kidney patterning genes disrupts renal morphogenesis. Development *133*, 569–578. https://doi.org/10.1242/dev.02220.
52. McFarlane, L., Truong, V., Palmer, J.S., and Wilhelm, D. (2013). Novel PCR assay for determining the genetic sex of mice. Sex Dev. *7*, 207–211. https://doi.org/10.1159/000348677.
53. Polański, K., Young, M.D., Miao, Z., Meyer, K.B., Teichmann, S.A., and Park, J.E. (2020). BBKNN: fast batch alignment of single cell transcriptomes. Bioinformatics *36*, 964–965. https://doi.org/10.1093/bioinformatics/btz625.
54. Wu, T., Hu, E., Xu, S., Chen, M., Guo, P., Dai, Z., Feng, T., Zhou, L., Tang, W., Zhan, L., et al. (2021). clusterProfiler 4.0: a universal enrichment tool for interpreting omics data. Innovation *2*, 100141. https://doi.org/10.1016/j.xinn.2021.100141.
55. Finak, G., McDavid, A., Yajima, M., Deng, J., Gersuk, V., Shalek, A.K., Slichter, C.K., Miller, H.W., McElrath, M.J., Prlic, M., et al. (2015). MAST: a flexible statistical framework for assessing transcriptional changes and characterizing heterogeneity in single-cell RNA sequencing data. Genome Biol. *16*, 278. https://doi.org/10.1186/s13059-015-0844-5.
56. Wolf, F.A., Angerer, P., and Theis, F.J. (2018). SCANPY: large-scale single-cell gene expression data analysis. Genome Biol. *19*, 15. https://doi.org/10.1186/s13059-017-1382-0.
57. Virtanen, P., Gommers, R., Oliphant, T.E., Haberland, M., Reddy, T., Cournapeau, D., Burovski, E., Peterson, P., Weckesser, W., Bright, J., et al. (2020). SciPy 1.0: fundamental algorithms for scientific computing in Python. Nat. Methods *17*, 261–272. https://doi.org/10.1038/s41592-019-0686-2.
58. Waskom, M. (2021). seaborn: statistical data visualization. J. Open Source Softw. *6*, 3021. https://doi.org/10.21105/joss.03021.
59. Butler, A., Hoffman, P., Smibert, P., Papalexi, E., and Satija, R. (2018). Integrating single-cell transcriptomic data across different conditions, technologies, and species. Nat. Biotechnol. *36*, 411–420. https://doi.org/10.1038/nbt.4096.
60. Nef, S., Schaad, O., Stallings, N.R., Cederroth, C.R., Pitetti, J.L., Schaer, G., Malki, S., Dubois-Dauphin, M., Boizet-Bonhoure, B., Descombes, P., et al. (2005). Gene expression during sex determination reveals a robust female genetic program at the onset of ovarian development. Dev. Biol. *287*, 361–377. https://doi.org/10.1016/j.ydbio.2005.09.008.
61. Zimmermann, C., Stévant, I., Borel, C., Conne, B., Pitetti, J.-L., Calvel, P., Kaessmann, H., Jégou, B., Chalmel, F., and Nef, S. (2015). Research resource: the dynamic transcriptional profile of Sertoli cells during the progression of spermatogenesis. Mol. Endocrinol. *29*, 627–642. https://doi.org/10.1210/me.2014-1356.
62. Stévant, I., Neirijnck, Y., Borel, C., Escoffier, J., Smith, L.B., Antonarakis, S.E., Dermitzakis, E.T., and Nef, S. (2018). Deciphering cell lineage specification during male sex determination with single-cell RNA sequencing. Cell Rep. *22*, 1589–1599. https://doi.org/10.1016/j.celrep.2018.01.043.
63. Stévant, I., Kühne, F., Greenfield, A., Chaboissier, M.-C., Dermitzakis, E.T., and Nef, S. (2019). Dissecting cell lineage specification and sex fate determination in gonadal somatic cells using single-cell transcriptomics. Cell Rep. *26*, 3272–3283.e3. https://doi.org/10.1016/J.CELREP.2019.02.069.
64. Sararols, P., Stévant, I., Neirijnck, Y., Rebourcet, D., Darbey, A., Curley, M.K., Kühne, F., Dermitzakis, E., Smith, L.B., and Nef, S. (2021). Specific transcriptomic signatures and dual regulation of steroidogenesis between fetal and adult mouse Leydig cells. Front. Cell Dev. Biol. *9*, 695546. https://doi.org/10.3389/fcell.2021.695546.
65. Mayère, C., Regard, V., Perea-Gomez, A., Bunce, C., Neirijnck, Y., Djari, C., Bellido-Carreras, N., Sararols, P., Reeves, R., Greenaway, S., et al. (2022). Origin, specification and differentiation of a rare supporting-like lineage in the developing mouse gonad. Sci. Adv. *8*, eabm0972. https://doi.org/10.1126/SCIADV.ABM0972.
66. Ademi, H., Djari, C., Mayère, C., Neirijnck, Y., Sararols, P., Rands, C.M., Stévant, I., Conne, B., and Nef, S. (2022). Deciphering the origins and fates of steroidogenic lineages in the mouse testis. Cell Rep. *39*, 110935. https://doi.org/10.1016/J.CELREP.2022.110935.
67. Neirijnck, Y., Calvel, P., Kilcoyne, K.R., Kühne, F., Stévant, I., Griffeth, R.J., Pitetti, J.L., Andric, S.A., Hu, M.C., Pralong, F., et al. (2018). Insulin and IGF1 receptors are essential for the development and steroidogenic function of adult Leydig cells. FASEB (Fed. Am. Soc. Exp. Biol.) J. *32*, 3321–3335. https://doi.org/10.1096/fj.201700769RR.
68. Livermore, C., Simon, M., Reeves, R., Stévant, I., Nef, S., Pope, M., Mallon, A.M., Wells, S., Warr, N., and Greenfield, A. (2020). Protection against XY gonadal sex reversal by a variant region on mouse chromosome 13. Genetics *214*, 467–477. https://doi.org/10.1534/genetics.119.302786.
69. Eicher, E.M., Washburn, L.L., Whitney, J.B., and Morrow, K.E. (1982). Mus poschiavinus Y chromosome in the C57BL/6J murine genome causes sex reversal. Science *217*, 535–537. https://doi.org/10.1126/science.7089579.
70. Traag, V.A., Waltman, L., and van Eck, N.J. (2019). From Louvain to Leiden: guaranteeing well-connected communities. Sci. Rep. *9*, 5233–5312. https://doi.org/10.1038/s41598-019-41695-z.

STAR★METHODS

KEY RESOURCES TABLE

REAGENT or RESOURCE	SOURCE	IDENTIFIER
Antibodies		
goat anti-GATA4	Santa Cruz Biotechnology Inc.	Cat#sc-1237; RRID:AB_2108747
chicken anti-GFP	Abcam	Cat#13970; RRID:AB_300798
rabbit anti-LEF1	Cell Signaling Technology	Cat#2230; RRID:AB_823558
mouse anti-NR5A1	R&D systems	Cat#PP-N1665-00; RRID:AB_2251509
Alexa Fluor 488 donkey anti-goat IgG	Invitrogen	Cat#A11055; RRID:AB_2534102
Alexa Fluor 555 donkey anti-mouse IgG	Invitrogen	Cat#A-31570; RRID:AB_2536180
Alexa Fluor 647 donkey anti-chicken IgY (igG)	Jackson ImmunoResearch Labs	Cat#703-605-155; RRID:AB_2340379
Alexa Fluor 647 donkey anti-rabbit IgG	Invitrogen	Cat#A-31573; RRID:AB_2536183
Chemicals, peptides, and recombinant proteins		
Papain dissociation system	Worthington	Cat#LK003150
DMEM	Gibco	Cat#11885084
Fetal bovine serum	Sigma-Aldrich	Cat# F2442
Draq7 Dye	Beckman Coulter	Cat#B25595
Trypsin-EDTA (0.05%), phenol red	Gibco	Cat#25300054
Opal 650 reagent pack	Akoya Biosciences	Cat#FP1496001KT
Normal donkey serum	Jackson ImmunoResearch	Cat#017-000-121
Hoechst 33,342	Invitrogen	Cat#H3570
Critical commercial assays		
Chromium Single Cell 3′ Reagent Kit v2	10x Genomics	Cat#PN-120237; PN-120236; PN-120262
Qubit fluorometric assay with dsDNA HS Assay Kit	Invitrogen	Cat#Q32851
High Sensitivity DNA Kit	Agilent	Cat#5067-4626
RNAscope® Multiplex Fluorescent Reagent Kit v2	Advanced Cell Diagnostics	Cat#323100
RNAscope®Probe -Mm-Nefm	Advanced Cell Diagnostics	Cat#315611
Deposited data		
Single-cell atlas of mouse early adrenogonadal development	This paper	GEO: GSE156176
Code for analysis	This paper	Zenodo: https://doi.org/10.5281/zenodo.7404773
Experimental models: Organisms/strains		
Mouse: Nr5a1^{Tg}: Tg(Nr5a1/EGFP)1Klp	Stallings et al.[14]	Cat#MGI:5493455
Oligonucleotides		
Primers for sex genotyping	McFarlane et al.[52]	N/A
Software and algorithms		
bbknn 1.5.0	Polański et al.[53]	https://bbknn.readthedocs.io/en/latest/; *RRID:SCR_022807*
Cell Ranger 2.1.1	10XGenomics	https://support.10xgenomics.com/single-cell-gene-expression/software/pipelines/latest/what-is-cell-ranger; RRID:SCR_017344
ClusterProfiler 4.4.1	Wu et al.[54]	https://github.com/YuLab-SMU/clusterProfiler; RRID:SCR_016884

(*Continued on next page*)

Continued

REAGENT or RESOURCE	SOURCE	IDENTIFIER
MAST 1.20	Finak et al.[55]	https://www.bioconductor.org/packages/release/bioc/html/MAST.html RRID:SCR_016340
Pandas 1.2.1	https://doi.org/10.5281/zenodo.3509134	https://pandas.pydata.org; RRID:SCR_018214
Python 3.6	Python Software Foundation	https://www.python.org; RRID:SCR_008394
R 4.1.2	The R core Team	https://www.r-project.org/; RRID:SCR_001905
Scanpy 1.8.2	Wolf et al.[56]	https://scanpy.readthedocs.io; RRID:SCR_018139
Scipy 1.6.0	Virtanen et al.[57]	https://scipy.org; RRID:SCR_008058
Seaborn 0.11.1	Waskom[58]	https://seaborn.pydata.org; RRID:SCR_018132
Seurat 2.3.4	Butler et al.[59]	https://satijalab.org/seurat/; RRID:SCR_016341
ZEN 2.6 (Blue Edition)	Zeiss	http://www.zeiss.com/microscopy/en_us/products/microscope-software/zen.html; RRID:SCR_013672

RESOURCE AVAILABILITY

Lead contact

Further information and requests for resources and reagents should be directed to and will be fulfilled by the lead contact Serge Nef (serge.nef@unige.ch).

Materials availability

All unique/stable reagents generated in this study are available from the lead contact with a completed Materials Transfer Agreement.

Data and code availability

Single-cell RNA-seq data have been deposited at GEO (GEO: GSE156176). All original code has been deposited at Zenodo (Zenodo: https://doi.org/10.5281/zenodo.7404773). Any additional information required to reanalyze the data reported in this paper is available from the lead contacts upon request.

EXPERIMENTAL MODEL AND SUBJECT DETAILS

All animal work was conducted according to the ethical guidelines of the Direction Générale de la Santé of the Canton de Genève (experimentation ID GE/57/18). *Nr5a1-eGFP*^{Tg} mouse strain was described previously[14] and has been maintained on a CD1 genetic background. This strain was chosen to allow better comparison with our previous work which used mixed or outbread strains[27,60–64,65,66,67] and to avoid sensitivity to disruption of testis determination that exists in pure genetic background such as C57BL/6N or C57BL/6J.[68,69] E9.0 (18 ± 3 somites), E10.5 (8 ± 2 tail somites (ts)), E11.5 (19 ± 4 ts) and E12.5 embryos from timed matings (day of vaginal plug = 0.5) were collected and the presence of the *Nr5a1-eGFP* transgene was assessed under UV light. Sexing of E9.0, E10.5 and E11.5 embryos was performed by PCR with a modified protocol from.[52] Each condition (organ, sex and developmental stage) was performed in two independent replicates.

METHODS DETAILS

Single cell suspension and library preparation

Posterior trunks, urogenital ridges and adrenal glands were enzymatically dissociated at 37°C between 30 and 40 min using the Papain dissociation system (Worthington LK003150). Cells were resuspended in DMEM (Gibco 11,885,084) supplemented with 2% fetal bovine serum (Sigma-Aldrich F2442), filtered through a 70 μm cell strainer and stained with Draq7 (Beckman Coulter B25595). Viable single cells were collected on a BD FACSAria II by excluding debris (side scatter *vs.* forward scatter), dead cells

(side scatter *vs.* Draq7 staining), and doublets (height *vs.* width). Testes and ovaries were enzymatically dissociated 10 min at 37°C using Trypsin-EDTA 0.05% (Gibco 25,300,054). After centrifugation and counting, 3000 to 7000 single cells were loaded on a 10x Chromium Controller (10x Genomics). Single-cell RNA-Seq libraries were prepared using the Chromium Single Cell 3′ Reagent Kit v2 (10x Genomics PN-120237 PN-120236 PN-120262) according to manufacturer's protocol.

Sequencing

Library quantification was performed using the Qubit fluorometric assay with dsDNA HS Assay Kit (Invitrogen Q32851). Library quality assessment was performed using a Bioanalyzer Agilent 2100 with a High Sensitivity DNA chip (Agilent 5067-4626). Libraries were diluted, pooled and sequenced on an Illumina HiSeq4000 using a paired-end, single index sequencing mode as follow: 26 base-pair (bp) Read1, 98 bp Read2 and 8 bp i7 index. Libraries were sequenced at a targeted depth of 100,000 to 150,000 reads per cell. Sequencing was performed at the Health 2030 Genome Center, Geneva.

Immunofluorescence and RNAscope analyses

Embryonic samples from timed matings (day of vaginal plug = E0.5) were collected and fixed overnight in 4% paraformaldehyde, serially dehydrated, embedded in paraffin, and 5-μm-thick transverse sections were prepared.

For dual *in situ* hybridization/immunofluorescence analyses, RNAscope for *Nefm* transcripts (RNAscope Probe - Mm-Nefm, Advanced Cell Diagnostics, Cat#315611) was performed with the RNAscope Multiplex Fluorescent Reagent Kit v2 (Advanced Cell Diagnostics, Cat# 323100) according to manufacturer's instructions. After developing HRP-C1 signal with Opal 650 dye (Akoya, Cat#FP1496001KT), sections were blocked for 2 h at room temperature, and primary antibodies incubated overnight at 4°C. Alexa Fluor-conjugated secondary antibodies were used (Thermo Fisher Scientific, Waltham, MA, USA). Slides were counterstained with Hoechst dye and mounted in PBS:glycerol (1:1).

For immunofluorescence analyses, paraffin sections were dewaxed and rehydrated*via* ethanol series. Antigen retrieval was performed in sodium citrate buffer (10 mM pH 6) for 2 min in a pressure cooker. Blocking, antibodies incubations, counterstain and slides mounting were performed as described above for dual *in situ* hybridization/immunofluorescence.

Primary antibodies and dilutions used in this study included the following: GATA4 (1:200, Santa Cruz Biotechnology Inc., Cat#sc-1237), GFP (1:200, Abcam, Cat#13970), LEF1 (1:300, Cell Signaling Technology, Cat#2230), NR5A1 (1:200, R&D systems, Cat#PP-N1665-00).

All images were acquired using Zeiss LSM780 microscopy at the PRISM Imaging Facility, and processed with Zen software (Carl Zeiss).

QUANTIFICATION AND STATISTICAL ANALYSIS

Single-cell RNA sequencing analysis

Demultiplexing, alignment, barcodes filtering, quality checks, data aggregation, gene filtering, normalization, and dimensionality reduction were performed as described in.[27]

Among the dataset, 39.2% (28,346) cells were from XX and 60.8% (43,927) from XY embryos, with 18.1% (13,060) from E9.0 samples, 20.7% (14,962) from E10.5, 23.1% (16,670) from E11.5 and 38.2% (27,581) from E12.5 (Figures S1C and S1D). Raw UMI counts were normalized for library size (normalize_per_cell function from Scanpy), log-transformed (log1p function from Scanpy) and normalized for sequencing depth (regress_out function on UMI count from Scanpy).

Genes detected in more than 50 cells (14,394 genes) were used to compute independent component analysis (ICA) using their normalized value (RunICA function from Seurat, nics = 100). Batch effect between replicates was corrected by computing the neighborhood graph with the BBKNN python package (version 1.4.0) (neighbors_within_batch = 3 and n_pcs = 100).[53] For visualization, the corrected neighborhood graph was embedded in two dimensions using UMAP[15] (umap function from Scanpy with default parameters), and used for cell clustering with the Leiden algorithm[70] (leiden function from Scanpy, resolution = 2.2).

To study AGP separation, we selected the 5,128 cells belonging to clusters 7 (CE adrenogonadal primordium), 17 (CE gonadal primordium) and 27 (adrenal primordium). We computed a force-directed graph (draw_graph function from Scanpy with default parameters) using previously computed corrected neighbor graph and ICA. A new clustering on this dataset was performed as described above using a resolution of 0.7.

For lineage reconstruction, connectivities between clusters were estimated (paga function from Scanpy with default parameters)[31] and pseudotime calculated (dpt function from Scanpy with default parameters and root cell assigned from subcluster 1). Cells were classified according to their assigned path (adrenal: subclusters 1, 3, 6, 2, 5; gonadal: subclusters 1, 3, 6, 4, 0) and ordered according to their pseudotime score. Genes differentially expressed between adrenal and gonadal lineages, and between subclusters in pairs, were computed with a MAST test (FindMarkers function from Seurat), resulting in 1,737 differentially expressed genes. Genes were grouped according to their expression similarities, allowing the identification of specific expression patterns along pseudotime by hierarchical clustering using spearman distance (k-means = 22, method = Ward.D2). Gene ontology enrichment analysis of biological processes was performed on each gene profile using ClusterProfiler (v4.1). Gene groups have been manually ordered to improve the visualization of the sequentially enriched profiles in either path.

For lineage reconstruction of the mesodermal derivatives, we removed erythroblasts/erythrocytes (clusters 44, 45, 49), hematopoietic progenitors (cluster 46), germ cells (clusters 5, 18, 25, 48), neural/sympathoadrenal cell types (clusters 28, 29, 31, 34, 41, 42, 47) and notochord (cluster 51), resulting in a dataset of 59,619 cells. Connectivities between clusters were estimated as described above using PAGA.

Transcriptomic atlas annotation

Differential expression analysis on the 52 clusters for the complete dataset, or on the 8 subclusters of the subset, was calculated with a Mann-Whitney-Wilcoxon test (FindAllMarkers function from Seurat). Cluster-specific or -enriched genes were cross referenced with published cell type markers (highlighted in yellow in Table S1). Cell type annotation was done based on marker gene expression, developmental age, sex and sample type.

ADDITIONAL RESOURCES

We provide an interactive web portal to explore our annotated single-cell adrenogonadal atlas (https://lmedapp731.unige.ch/dataset02/). This provides researchers the possibility to query for their genes of interest per cell types, age, and sex.